Supplementary Information for:

Few-layer MoS_2 nanosheets with and without silicon nanoparticles as anodes for lithium-ion batteries

Ifra Marriam[ab]*, Mike Tebyetekerwa[c], Hao Chen[a], Hiran Chathuranga[ab], Nunzio Motta[bd], Jose A. Alarco[bd], Zhen-Jiang He[e], Jun-Chao Zheng[e], Aijun Du[bd], and Cheng Yan[ab]*.

[a.] *School of Mechanical, Medical, and Process Engineering, Faculty of Engineering, Queensland University of Technology, 2 George Street, Brisbane, QLD 4000, Australia.*
[b.] *Centre for Materials Science, Queensland University of Technology, 2 George Street, Brisbane, QLD 4000, Australia.*
[c.] *Dow Centre for Sustainable Engineering Innovation, School of Chemical Engineering, The University of Queensland, St. Lucia, Brisbane, QLD 4072 Australia.*
[d.] *School of Chemistry and Physics, Queensland University of Technology, 2 George Street, Brisbane, QLD 4000, Australia.*
[e.] *School of Metallurgy and Environment, Central South University, Changsha, Hunan 410083, China.*
**Corresponding authors.*
Email: ifra.marriam@hdr.qut.edu.au and c2yan@qut.edu.au

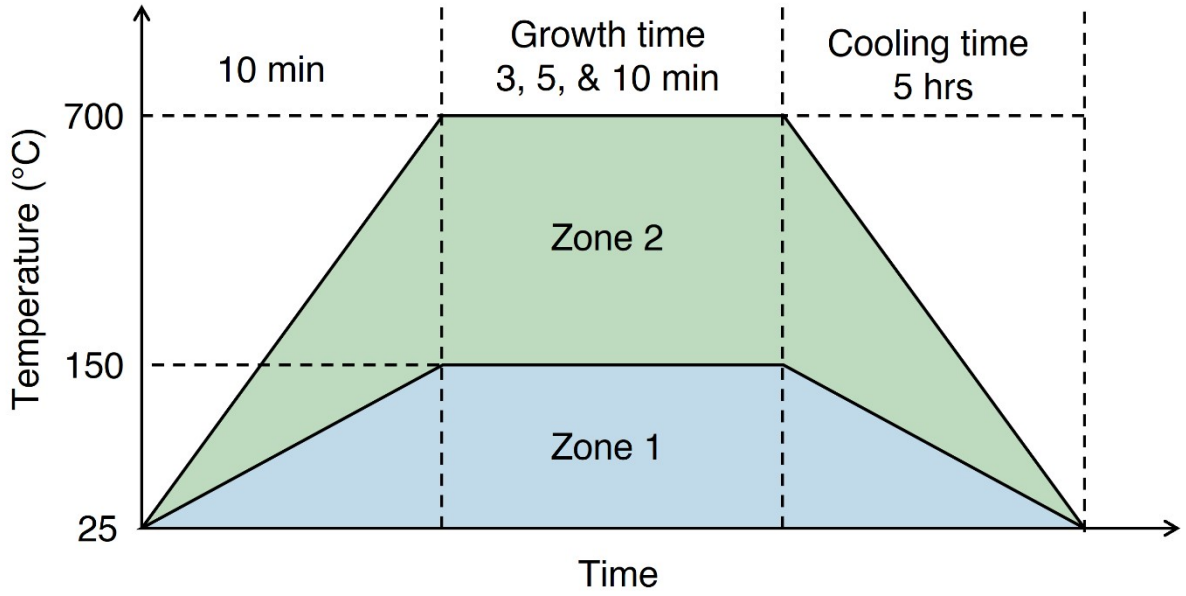

Figure S1. Temperature control during the growth of MoS_2 nanosheets. The CVD process of the MoS_2 took place in *a* two-zone furnace where the temperature of zone 1 was set to 150 °C for sulphur and zone 2 was set to 700 °C for MoO_3/NaCl. To control the reaction and to prevent sulphur from evaporating before the reaction, *the* sulphur sample boat was placed away from the temperature zone so that it does not start melting immediately. Sulphur was then inserted *in*to the heating area with the help of magnets once the temperature of zone 2 reached 700 °C. Once the temperatures of both zones reached the required values, the reaction took place and the temperatures were kept steady for 3, 5, and 10 minutes for MoS_2 growth to take place.

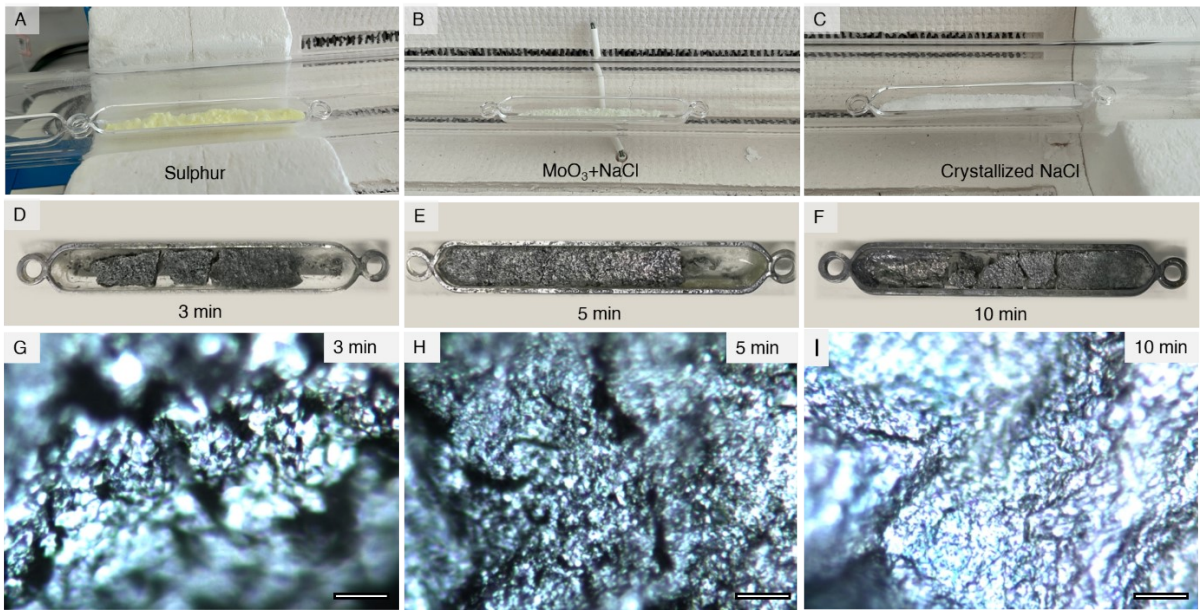

Figure S2. The photographs of the sample boats containing; (A) sulphur powder, B) MoO_3+NaCl, C) crystallized NaCl before CVD and D-F) MoS_2@NaCl after CVD process. (G-I) Optical Images of MoS_2@NaCl after CVD process (Scale bar = 25 um).

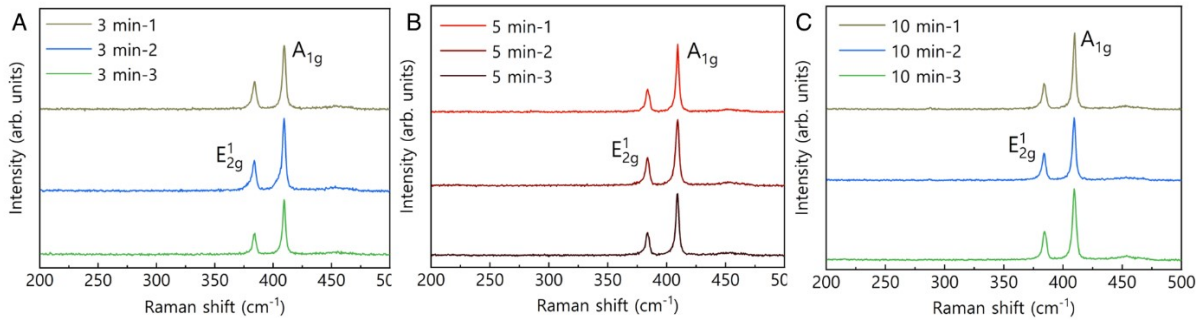

Figure S3. Raman spectroscopy of different samples after (A) 3 min, (B) 5 min, and (C) 10 min of growth time.

Synthesis of MoS_2 on Si via CVD

In another setup, for a rapid process, we also attempted to grow MoS_2 nanosheets directly onto the Si nanoparticles. The Si powder was used as a substrate instead of NaCl in the CVD process. But the Si powder is very light in weight which tends to fly off during CVD with the gas flow. Even though we obtained low Raman intensity peaks, which confirmed the presence of MoS_2 on Si (Figure S4A), but there were no observable MoS_2 2D nanosheets in the SEM images (Figure S4B and C). We attribute this to the smaller surface area of Si nanoparticles, which impedes the lengthwise growth of 2D MoS_2 nanosheets. Hence, the earlier prepared sandwiched heterostructure of MoS_2@Si was the best option.

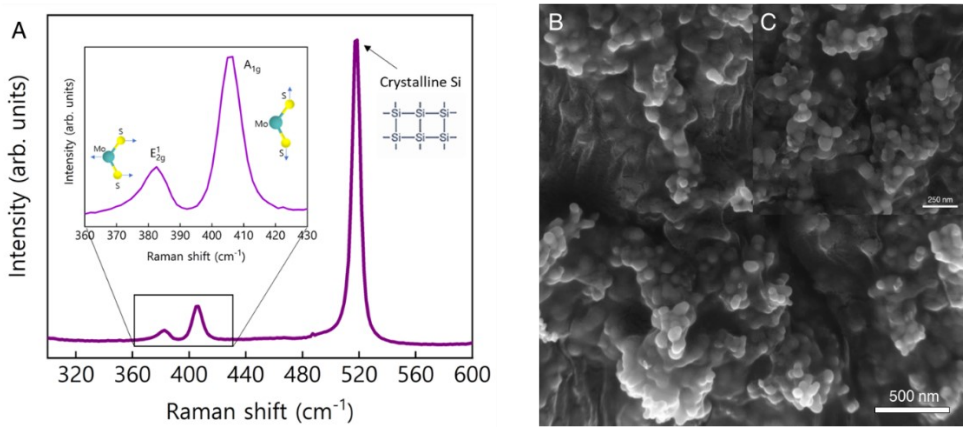

Figure S4. (A) Raman spectroscopy of MoS2 on Si powder and (B) The SEM image of MoS_2 on Si powder with its zoom in (C).

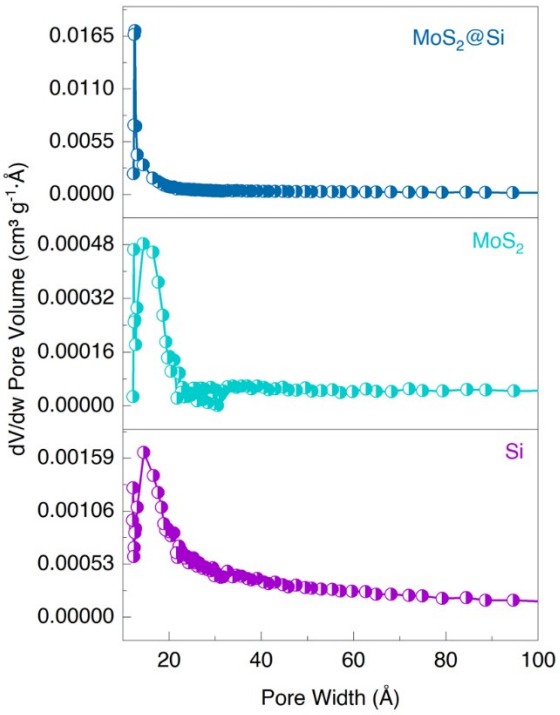

Figure S5. The pore size distribution of MoS_2@Si, MoS_2, and Si.

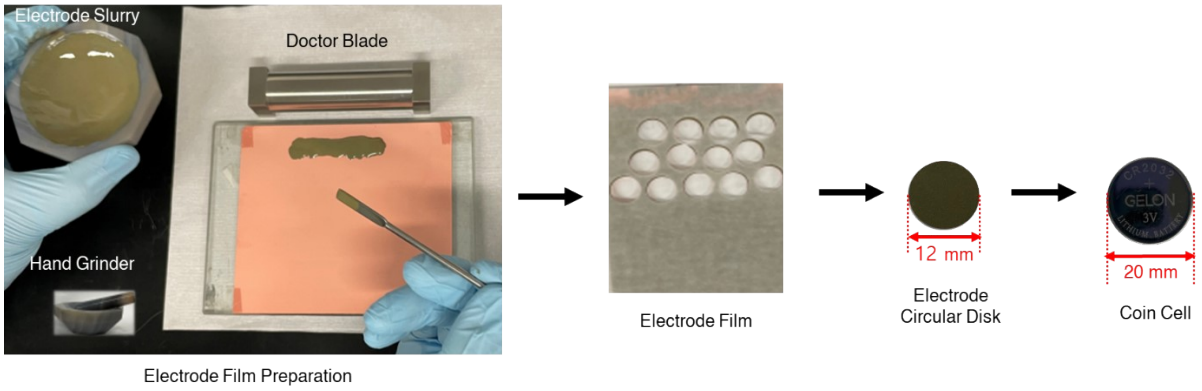

Figure S6. The photographs showing the preparation method of electrode slurry and coin cells for battery testing.

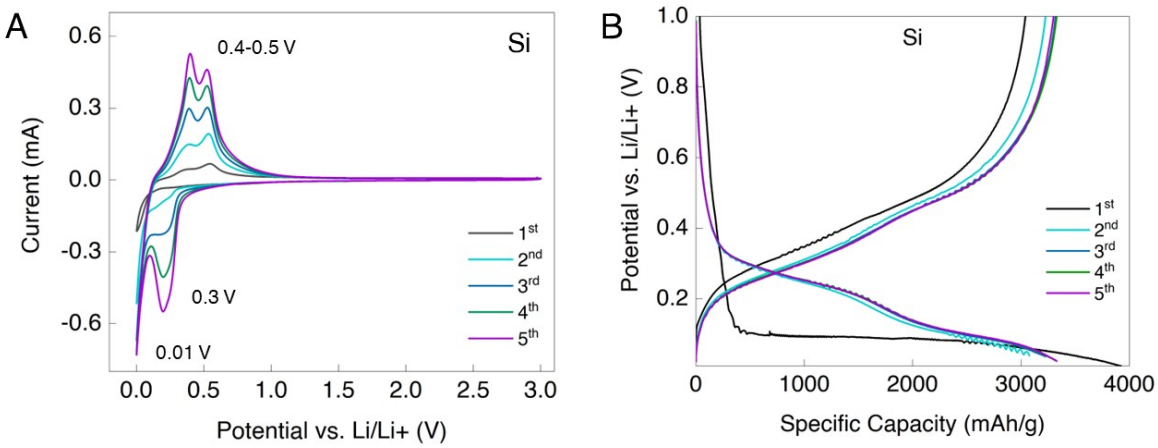

Figure S7. The electrochemical results. (A) CV curve of Si at a scan rate of 0.1 mV/s within the potential window of 0.01-3.0 V. (B) Galvanostatic charge/discharge profile of the initial five cycles for Si at 100 mA/g.

Table S1. The discharge and charge capacities of the MoS_2 and MoS_2@Si electrodes at different current densities.

	MoS_2		**MoS_2@Si**	
Current Densities (mA/g)	Discharge Capacities (mAh/g)	Charge Capacities (mAh/g)	Discharge Capacities (mAh/g)	Charge Capacities (mAh/g)
100	890	871	2331	2254
200	854	830	1865	1744
300	820	799	1456	1406
500	768	746	1087	1065
1000	508	454	625	612
500	668	700	1095	1058
300	780	779	1231	1193
200	856	847	1303	1260
100	911	904	1707	1658

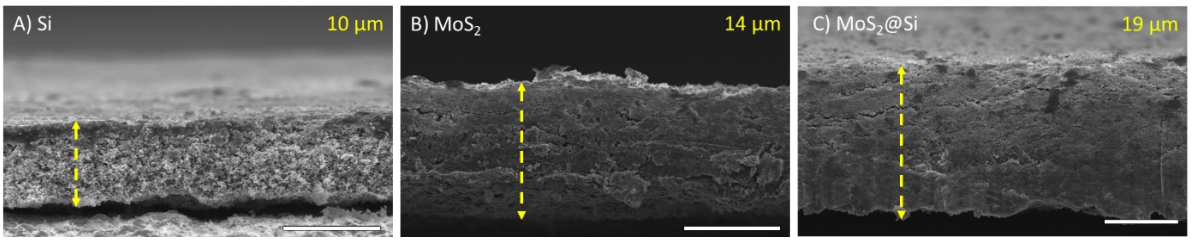

Figure S8. Cross-sectional SEM images of the electrodes before cyclic testing (scale bar= 10 µm).

Table S2. Comparison of volume expansion and electrochemical performance of Si anodes in Li-ion batteries.

Materials	Volume expansion (%)	Electrochemical Performance	No. Of cycles	Ref.
MoS_2@Si	68	993 mAh/g at 500 mA/g	500	This work
Si/graphene	72	714 mAh/g at 1000 mA/g	400	[1]
Si-Cr_3C_2@few-layer graphene	70	881.8 mAh/g at 1000 mA/g	300	[2]
SiO_x/Lignin	160	~900 mAh/g at 200 mA/g	250	[3]
Mesoporous Si/C microspheres	85	990 mAh/g at 100 mA/g	1000	[4]

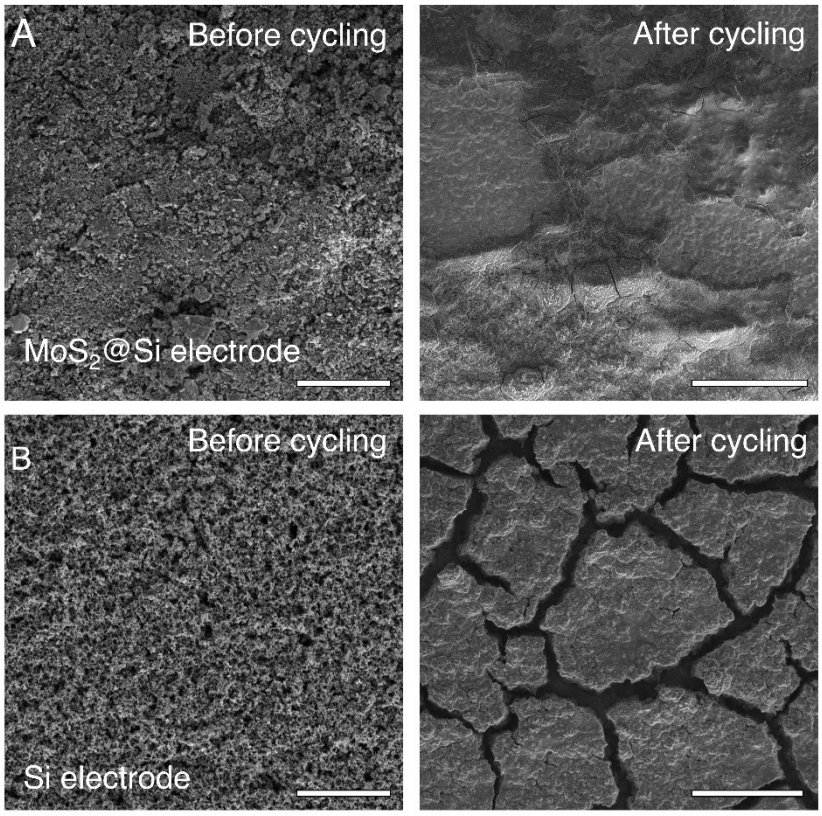

Figure S9. Ex-situ analysis of (A) MoS_2@Si and (B) Si electrodes before and after cycling.

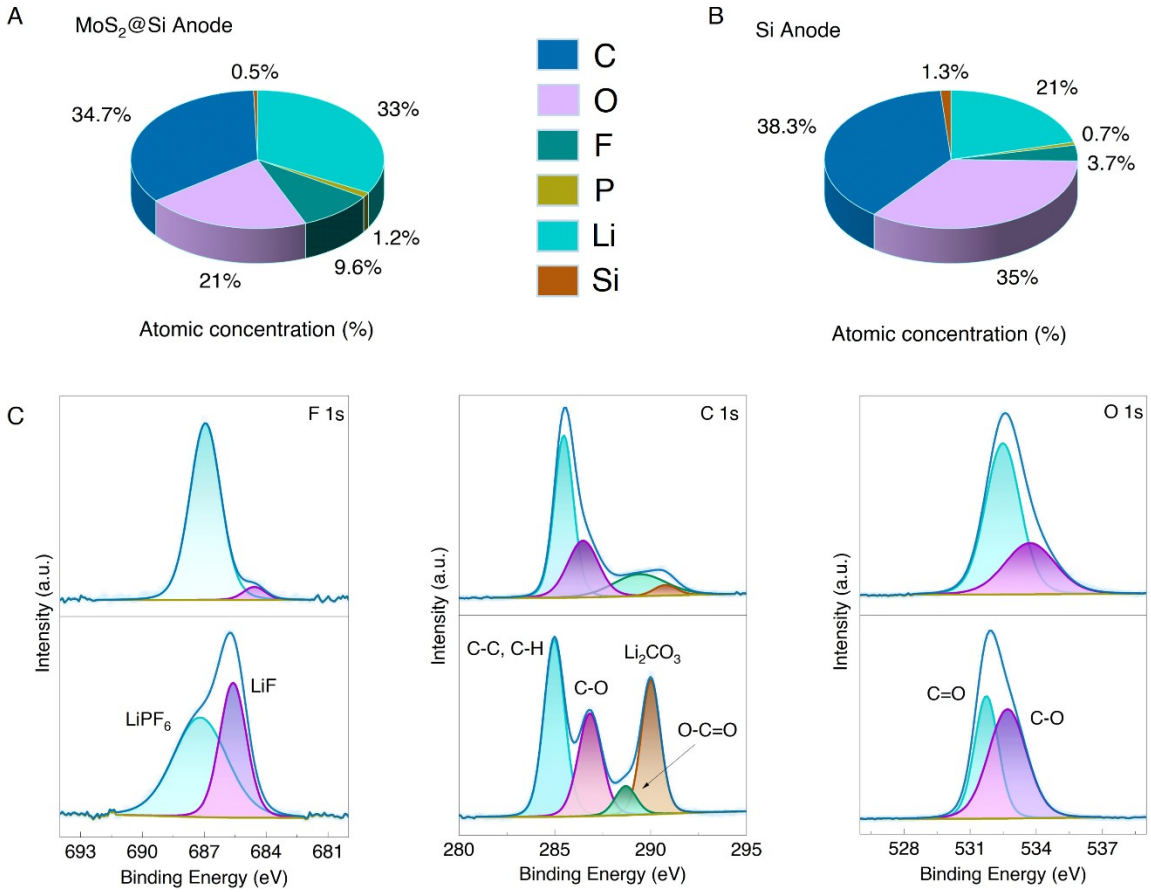

Figure S10. SEI analysis of Si and MoS_2@Si anodes using XPS Spectra. Atomic concentrations of A) MoS_2@Si and B) Si anodes after 500 cycles of charging/discharging at 500 mA/g. C) High-resolution XPS spectra of F 1s, C 1s, and O 1s. Si-top panel and MoS_2@Si bottom panel.

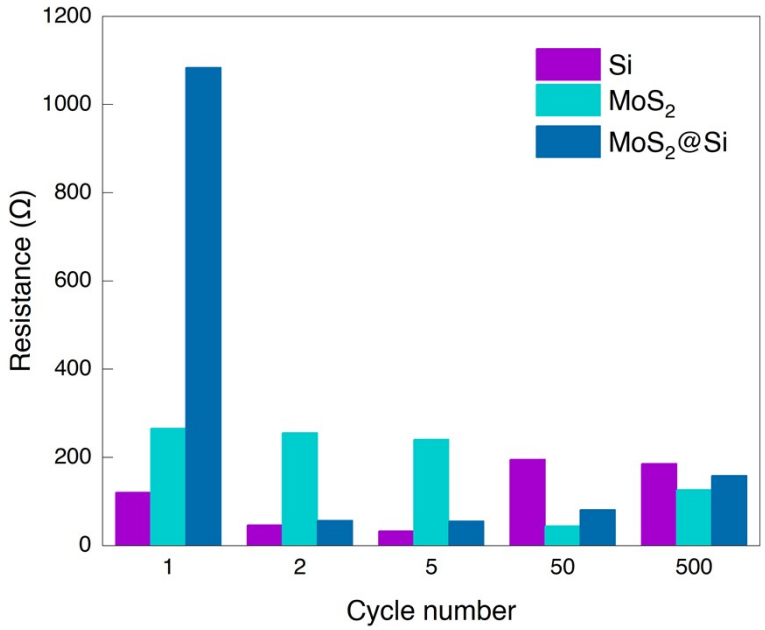

Figure S11. Evolution of the charge transfer resistance of the Si, MoS_2, and MoS_2@Si electrode from GCD discharge curves for cycles 1, 2, 5, 50, and 500 at 500 mA/g.

Supplementary Information References

1. H. Liu, W. Yang, S. Che, Y. Li, C. Xu, X. Wang, G. Ma, G. Huang and Y. Li, *Carbon*, 2022, **196**, 633-638.
2. Y. Liu, W. Sun, X. Lan, R. Hu, J. Cui, J. Liu, J. Liu, Y. Zhang and M. Zhu, *ACS Appl. Mater. Interfaces*, 2019, **11**, 38727-38736.
3. T. Chen, J. Hu, L. Zhang, J. Pan, Y. Liu and Y.-T. Cheng, *J. Power Sources*, 2017, **362**, 236-242.
4. Z.-L. Xu, Y. Gang, M. A. Garakani, S. Abouali, J.-Q. Huang and J.-K. Kim, *J. Mater. Chem. A*, 2016, **4**, 6098-6106.